

The single-degenerate channel for the progenitor of type Ia supernovae with different metallicities

X. Meng^{1,2} ^{*}, X. Chen¹ and Z. Han¹

¹ *National Astronomical Observatories/Yunnan Observatory, the Chinese Academy of Sciences, Kunming, 650011, China, conson859@msn.com*

² *Department of Physics and Chemistry, Henan Polytechnic University, Jiaozuo, 454000, China*

Accepted. Received

ABSTRACT

The single-degenerate channel for the progenitors of type Ia supernovae (SNe Ia) are currently accepted, in which a carbon-oxygen white dwarf (CO WD) accretes hydrogen-rich material from its companion, increases its mass to the Chandrasekhar mass limit, and then explodes as a SN Ia. Incorporating the prescription of Hachisu et al. (1999a) for the accretion efficiency into Eggleton’s stellar evolution code and assuming that the prescription is valid for *all* metallicities, we performed binary stellar evolution calculations for more than 25,000 close WD binaries with metallicities $Z = 0.06, 0.05, 0.04, 0.03, 0.02, 0.01, 0.004, 0.001, 0.0003$ and 0.0001 . For our calculations, the companions are assumed to be unevolved or slightly evolved stars (WD + MS). As a result, the initial parameter spaces for SNe Ia at various Z are presented in orbital period-secondary mass ($\log P_1, M_2^i$) planes. Our study shows that both the initial mass of the secondary and the initial orbital period increase with metallicity. Thus, the minimum mass of the CO WD for SNe Ia decreases with metallicity Z . The difference of the minimum mass may be as large as $0.24 M_\odot$ for different Z .

Adopting the results above, we studied the birth rate of SNe Ia for various Z via a binary population synthesis approach. If a single starburst is assumed, SNe Ia occur systemically earlier and the peak value of the birth rate is larger for a high Z . The Galactic birth rate from the WD + MS channel is lower than (but comparable to) that inferred from observations. Our study indicates that supernovae like SN2002ic would not occur in extremely low-metallicity environments, if the delayed dynamical-instability model in Han & Podsiadlowski (2006) is appropriate.

Key words: binaries:close-stars:evolution-supernovae:general-white dwarfs

1 INTRODUCTION

Type Ia supernovae (SNe Ia) play an important role in astrophysics, especially in cosmology. They appear to be good cosmological distance indicators and are successfully applied to determine cosmological parameters (e.g. Ω and Λ ; Riess et al. 1998; Perlmutter et al. 1999). There is a linear relation between the absolute magnitude of SNe Ia at maximum light and the magnitude drop of B light curve during the first 15 days following maximum. This relation is now known as **the** Phillips relation (Phillips 1993) and **is** adopted when SNe Ia **are used** as distance indicators. In this case, the Phillips relation is assumed to be valid at high redshift, although it comes from low-redshift samples. Obviously, this assumption is precarious since the exact nature of SNe Ia is still unclear (see the reviews by Hillebrandt & Niemeyer

2000; Leibundgut 2000). If the properties of SNe Ia evolve with redshift, the results for cosmology might be different. Thus, it is necessary to study the properties of SNe Ia at high redshift. Since metallicity may represent redshift to some extent (e.g. metallicity decreases with redshifts), it is a good method to study the properties of SNe Ia at various redshift by finding correlations between their properties and metallicity.

It is generally agreed that SNe Ia originate from the thermonuclear runaway of a carbon-oxygen white dwarf (CO WD) in a binary system. The CO WD accretes material from its companion, increases mass to its maximum stable mass, and then explodes as a thermonuclear runaway. Almost half of the WD mass is converted into radioactive nickel-56 in the explosion (Branch 2004), and the amount of nickel-56 determines the maximum luminosity of SNe Ia (Arnett 1982). Some numerical and synthetical results showed that metallicity has an effect on the final amount of nickel-56,

^{*} E-mail: conson859@msn.com

and thus the maximum luminosity (Timmes et al. 2003; Travaglio et al. 2005; Podsiadlowski et al. 2006). There is also some other evidence of the correlation between the properties of SNe Ia and metallicity from observations, e.g. Branch & Bergh 1993; Hamuy et al. 1996; Wang et al. 1997; Cappellaro et al. 1997; Shanks et al. 2002.

Although the fact that SNe Ia originate from the thermonuclear disruption of mass accreting white dwarfs is widely accepted, the precise nature of the progenitor systems remains unclear. According to the nature of the companions of the mass accreting white dwarfs, two competing scenarios have been proposed, i.e. the double-degenerate channel (DD, Iben & Tutukov 1984; Whelan & Iben 1987) and the single degenerate channel (SD, Whelan & Iben 1973; Nomoto, Thielemann & Yokoi 1984). In the DD channel, two CO WDs with a total mass larger than the Chandrasekhar mass limit may coalesce, and then explode as a SN Ia. Although the channel is theoretically less favored, e.g. double WD mergers may lead to accretion-induced collapses rather than to SNe Ia (Hillebrandt & Niemeyer 2000), it is premature to exclude the channel at present since there exists evidence that the channel may contribute a few SNe Ia (Howell et al. 2006; Branch 2006; Quimby, Höflich & Wheeler 2007). The single-degenerate Chandrasekhar model is the most widely accepted one at present (Whelan & Iben 1973; Nomoto, Thielemann & Yokoi 1984). In this model, the maximum stable mass of a CO WD is $\sim 1.378 M_{\odot}$ (close to the Chandrasekhar mass, Nomoto, Thielemann & Yokoi 1984), and the companion is probably a main sequence star or a slightly evolved star (WD+MS), or a red-giant star (WD+RG) (Yungelson et al. 1995; Li & van den Heuvel 1997; Hachisu et al. 1999a,b; Nomoto et al. 1999; Langer et al. 2000; Han & Podsiadlowski 2004). The SD model is supported by some observations. For example, variable **circumstellar** absorption lines were observed in the spectra of SN Ia 2006X (Patat et al. 2007), which indicates the SD nature of its precursor. Patat et al. (2007) suggested that the progenitor of SN 2006X is a WD + RG system based on the expansion velocity of the **circumstellar** material, while Hachisu et al. (2008) argued a WD + MS nature for this SN Ia. Recently, Voss & Nelemans (2008) suggested that SN 2007on is also possibly from a WD + MS channel. Moreover, several WD + MS systems are possible progenitors of SN Ia. For example, supersoft X-ray sources (SSSs) were suggested as good candidates for the progenitors of SNe Ia (Hachisu & Kato 2003a,b). Some of the SSSs are WD + MS systems and some are WD + RG systems (Di Stefano & Kong 2003). A direct way to confirm the progenitor model is to search for the companion stars of SNe Ia in their remnants. The discovery of the potential companion of Tycho's supernova may have verified the reliability of the WD + MS model (Ruiz-Lapuente et al. 2004; Ihara et al. 2007). In this paper, we only focus on the WD + MS channel, which is a very important channel for producing SNe Ia in the Galaxy (Han & Podsiadlowski 2004).

There are two problems for the WD + MS channel when confronted with observations, which are the absence of H in the vast majority of SNe Ia spectra and the difficulty of producing SNe Ia with long delay times (older than 10 Gyr inferred from SNe Ia in elliptical galaxies in the lo-

cal universe, Mannucci et al. 2005) or extremely short delay times (shorter than 0.1 Gyr, Mannucci et al. 2006). The absence of H in the spectra likely implies that the density of circumstellar material (CSM) around SNe Ia is very low or the amount of the hydrogen-rich material stripped from the companion is very small (Mattila et al. 2005; Leonard 2007). Neither of the two problems can be overcome easily in the WD + MS channel. We know from observations that some SNe Ia have delay times longer than 10 Gyr or shorter than 0.1 Gyr (Scannapieco & Bildsten 2005; Mannucci et al. 2006; Totani et al. 2008), but the WD + MS channel can only account for SNe Ia with delay times shorter than 2 Gyr while longer than 0.1 Gyr (Han & Podsiadlowski 2004). It is likely that SNe Ia with long or short delay times come from other channels than the WD + MS channel, e.g. SNe Ia with long delay times come from WD + RG channel, while those with short delay times come from a WD + He star channel (Wang, Meng, Chen & Han 2008, in preparation).

Many works have concentrated on the WD+MS channel. Hachisu et al. (1999a,b, 2008) and Nomoto et al. (1999, 2003) have studied the WD+MS channel by a simple analytical method for treating binary interactions. Such analytic prescriptions, as pointed out by Langer et al. (2000), can not describe some mass-transfer phases, especially those occurring on a thermal time-scale. Li & van den Heuvel (1997) studied this channel from detailed binary evolution calculation, while two WD masses, 1.0 and 1.2 M_{\odot} , are considered. Langer et al. (2000) investigated the channel for metallicities $Z = 0.001$ and 0.02, but only for mass transfer during core hydrogen burning phase (case A). Han & Podsiadlowski (2004) carried out a detailed study of the channel including case A and early case B (mass transfer occurs at Hertzsprung gap (HG)) for $Z = 0.02$. Considering that not all SNe Ia are found in solar metallicity environments, we pay attention to the correlation between the properties of SNe Ia and metallicities here.

In this paper, we study the WD + MS channel comprehensively and systematically at various Z , showing the parameter spaces for the progenitors of SNe Ia and the distributions of the initial parameters for the progenitors of SNe Ia. The results can be **effectively** used in binary population synthesis, or be helpful to search for the potential progenitor systems of SNe Ia. In section 2, we simply describe the numerical code for binary evolution calculations and the grid of binary models we have calculated. The evolutionary results are shown in section 3. We describe the binary population synthesis (BPS) method in section 4 and present the BPS results in section 5. In section 6, we briefly discuss our results, and finally we summarize the main results in section 7.

2 BINARY EVOLUTION CALCULATION

We use the stellar evolution code of Eggleton (1971, 1972, 1973) to calculate the binary evolutions of WD+MS systems. The code has been updated with the latest input physics over the last three decades (Han, Podsiadlowski & Eggleton 1994; Pols et al. 1995, 1998). Roche lobe overflow (RLOF) is treated within the code described by Han et al. (2000). We set the ratio of mixing length to local pressure scale height, $\alpha = l/H_p$, to 2.0,

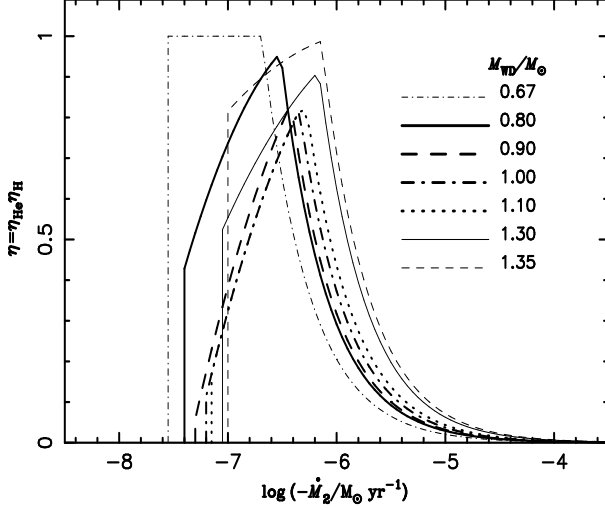


Figure 1. The total accumulation efficiency, $\eta = \eta_{\text{He}}\eta_{\text{H}}$, as a function of mass-transfer rate, $|\dot{M}_2|$. The hydrogen mass fraction, $X = 0.7$, is adopted for the critical accretion rate, \dot{M}_{cr} .

and set the convective overshooting parameter, δ_{OV} , to 0.12 (Pols et al. 1997; Schröder et al. 1997), which roughly corresponds to an overshooting length of $0.25H_{\text{P}}$. Ten metallicities are adopted here (i.e. $Z = 0.0001, 0.0003, 0.001, 0.004, 0.01, 0.02, 0.03, 0.04, 0.05$ and 0.06). The opacity tables for these metallicities are compiled by Chen & Tout (2007) from Iglesias & Rogers (1996) and Alexander & Ferguson (1994). For each Z , the initial hydrogen mass fraction is obtained by

$$X = 0.76 - 3.0Z, \quad (1)$$

(Pols et al. 1998). Based on the correlation among X , Y and Z used here, Pols et al. (1998) well reproduced the color-magnitude diagram (CMD) of some clusters.

Instead of solving stellar structure equations of a WD, we adopt the prescription of Hachisu et al. (1999a) on WDs accreting hydrogen-rich material from their companions. The following is a brief introduction of this prescription. In the WD + MS channel, the companion fills its Roche lobe at MS or during HG, and transfers material onto the WD. If the mass-transfer rate, $|\dot{M}_2|$, exceeds a critical value, \dot{M}_{cr} , we assume that the accreted hydrogen steadily burns on the surface of WD and that the hydrogen-rich material is converted into helium at the rate of \dot{M}_{cr} . The unprocessed matter is assumed to be lost from the system as an optically thick wind at a rate of $\dot{M}_{\text{wind}} = |\dot{M}_2| - \dot{M}_{\text{cr}}$ (Hachisu et al. 1996). Based on the opacity from Iglesias & Rogers (1996), the optically thick wind is very sensitive to Fe abundance, and it is likely that the wind does not work when Z is lower than a certain value (i.e. $Z < 0.002$, Kobayashi et al. 1998). Thus, there should be an obvious low-metallicity threshold for SNe Ia in comparison with SN II. However, this metallicity threshold has not been found (Prieto et al. 2008). Considering the uncertainties in the opacities, we therefore assume rather arbitrarily that the optically thick wind is still valid for low metallicities.

The critical accretion rate is

$$\dot{M}_{\text{cr}} = 5.3 \times 10^{-7} \frac{(1.7 - X)}{X} (M_{\text{WD}} - 0.4), \quad (2)$$

where X is hydrogen mass fraction and M_{WD} is the mass of the accreting WD (mass is in M_{\odot} and mass-accretion rate is in M_{\odot}/yr , Hachisu et al. 1999a). We have not included the effect of metallicities on equation (2) since the effect is very small and can be neglected (Meng et al. 2006).

The following assumptions are adopted when $|\dot{M}_2|$ is smaller than \dot{M}_{cr} . (1) When $|\dot{M}_2|$ is higher than $\frac{1}{2}\dot{M}_{\text{cr}}$, the hydrogen-shell burning is steady and no mass is lost from the system. (2) When $|\dot{M}_2|$ is lower than $\frac{1}{2}\dot{M}_{\text{cr}}$ but higher than $\frac{1}{8}\dot{M}_{\text{cr}}$, a very weak shell flash is triggered but no mass is lost from the system. (3) When $|\dot{M}_2|$ is lower than $\frac{1}{8}\dot{M}_{\text{cr}}$, the hydrogen-shell flash is so strong that no material is accumulated on the surface of the CO WD. We define the growth rate of the mass of the helium layer under the hydrogen-burning shell as

$$\dot{M}_{\text{He}} = \eta_{\text{H}}|\dot{M}_2|, \quad (3)$$

where η_{H} is the mass accumulation efficiency for hydrogen burning. According to the assumptions above, the values of η_{H} are:

$$\eta_{\text{H}} = \begin{cases} \dot{M}_{\text{cr}}/|\dot{M}_2|, & |\dot{M}_2| > \dot{M}_{\text{cr}}, \\ 1, & \dot{M}_{\text{cr}} \geq |\dot{M}_2| \geq \frac{1}{8}\dot{M}_{\text{cr}}, \\ 0, & |\dot{M}_2| < \frac{1}{8}\dot{M}_{\text{cr}}. \end{cases} \quad (4)$$

Helium is ignited when a certain amount of helium is accumulated. If a He-flash occurs, some of the helium is blown off from the surface of the CO WD. Then, the mass growth rate of the CO WD, \dot{M}_{WD} , is

$$\dot{M}_{\text{WD}} = \eta_{\text{He}}\dot{M}_{\text{He}} = \eta_{\text{He}}\eta_{\text{H}}|\dot{M}_2|, \quad (5)$$

where η_{He} is the mass accumulation efficiency for helium-shell flashes, and its value is taken from Kato & Hachisu (2004):

$$\eta_{\text{He}} = 1, \quad (6)$$

for $M_{\text{WD}} < 0.8M_{\odot}$.

$$\eta_{\text{He}} = \begin{cases} -0.35(\log \dot{M}_{\text{He}} + 6.1)^2 + 1.02, & \log \dot{M}_{\text{He}} < -6.34, \\ 1, & \log \dot{M}_{\text{He}} \geq -6.34, \end{cases} \quad (7)$$

for $0.8M_{\odot} \leq M_{\text{WD}} < 0.9M_{\odot}$.

$$\eta_{\text{He}} = \begin{cases} -0.35(\log \dot{M}_{\text{He}} + 5.6)^2 + 1.07, & \log \dot{M}_{\text{He}} < -6.05, \\ 1, & \log \dot{M}_{\text{He}} \geq -6.05, \end{cases} \quad (8)$$

for $0.9M_{\odot} \leq M_{\text{WD}} < 1.0M_{\odot}$.

$$\eta_{\text{He}} = \begin{cases} -0.35(\log \dot{M}_{\text{He}} + 5.6)^2 + 1.01, & \log \dot{M}_{\text{He}} < -5.93, \\ 1, & \log \dot{M}_{\text{He}} \geq -5.93, \end{cases} \quad (9)$$

for $1.0M_{\odot} \leq M_{\text{WD}} < 1.1M_{\odot}$.

$$\eta_{\text{He}} = \begin{cases} 0.54 \log \dot{M}_{\text{He}} + 4.16, & \log \dot{M}_{\text{He}} < -5.95, \\ -0.54(\log \dot{M}_{\text{He}} + 5.6)^2 + 1.01, & -5.95 \leq \log \dot{M}_{\text{He}} < -5.76, \\ 1, & \log \dot{M}_{\text{He}} \geq -5.76, \end{cases} \quad (10)$$

for $1.1M_{\odot} \leq M_{\text{WD}} < 1.3M_{\odot}$.

$$\eta_{\text{He}} = \begin{cases} -0.175(\log \dot{M}_{\text{He}} + 5.35)^2 + 1.03, & \log \dot{M}_{\text{He}} < -5.83, \\ 1, & \log \dot{M}_{\text{He}} \geq -5.83, \end{cases} \quad (11)$$

for $1.3M_{\odot} \leq M_{\text{WD}} < 1.35M_{\odot}$.

$$\eta_{\text{He}} = \begin{cases} -0.115(\log \dot{M}_{\text{He}} + 5.7)^2 + 1.01, & \log \dot{M}_{\text{He}} < -6.05, \\ 1, & \log \dot{M}_{\text{He}} \geq -6.05, \end{cases} \quad (12)$$

for $M_{\text{WD}} \geq 1.35M_{\odot}$.

We show the total accumulation efficiency, $\eta = \eta_{\text{He}}\eta_{\text{H}}$, as a function of mass transfer rate in Fig. 1, which clearly shows the prescription above. We incorporated this prescription into Eggleton's stellar evolution code and followed the evolutions of both the mass donor and the accreting CO WD. The mass lost from the system is assumed to take away the specific orbital angular momentum of the accreting WD. We calculated more than 25,000 WD+MS binary systems with various metallicities, and obtained a large, dense model grid. The initial masses of donor stars, M_2^i , range from $0.8 M_{\odot}$ to $4.3 M_{\odot}$; the initial masses of CO WDs, M_{WD}^i , from $0.629 M_{\odot}$ to $1.20 M_{\odot}$; the initial orbital periods of binary systems, P^i , from the minimum value (at which a zero-age main-sequence (ZAMS) star fills its Roche lobe) to ~ 20 days, where the companion star fills its Roche lobe at the end of the HG. In the calculations, we assume that the WD explodes as a SN Ia when its mass reaches the Chandrasekhar mass limit, i.e. $1.378 M_{\odot}$ (Nomoto, Thielemann & Yokoi 1984).

3 BINARY EVOLUTION RESULTS

3.1 Initial parameters for the progenitor of SNe Ia

To conveniently compare our results with previous studies in the literature, we summarize the final outcomes of all the binary evolution calculations in the initial orbital period-secondary mass ($\log P^i, M_2^i$) plane. For the size limit of this paper we only show two examples from the ends of the metallicity range we explored (i.e. $Z = 0.06$ and $Z = 0.0001$) in Figs. 2 and 3. One can download all the figures from <http://www.ynao.ac.cn/~bps/download/xiangcunmeng.htm>.

From the two figures, we see that CO WDs may reach a mass of $1.378 M_{\odot}$ during the optically thick wind phase (the filled squares) or after optically thick wind while in stable (the filled circles) or unstable (the filled triangles) hydrogen-burning phase. All these systems are probably progenitors of SNe Ia. Due to strong hydrogen-shell flash or dynamically unstable mass transfer, many CO WDs fail to reach $1.378 M_{\odot}$. Among them, some CO WDs have mass larger than $1.30 M_{\odot}$ at the onset of dynamically unstable mass transfer (filled stars). These CO WDs still have a chance to increase their masses to $1.378 M_{\odot}$ through delayed dynamical instability (Han & Podsiadlowski 2006) and become SNe Ia. These systems are possible progenitors of the SN 2002ic-like supernovae (Han & Podsiadlowski 2006). The delayed dynamical instability can successfully explain many properties of SN 2002ic (Han & Podsiadlowski 2006), but more evidence is necessary to confirm this scenario. Thus, we have not included them in the contours of initial parameter space for SNe Ia (Fig 2).

For the contours, the left boundaries are determined by the radii of ZAMS stars, i.e. Roche lobe overflow (RLOF) starts at zero age, while the systems beyond the right boundaries undergo dynamically unstable mass transfer at the

base of the red giant branch (RGB)¹. The upper boundaries are determined by the delayed dynamical instability (mainly for $Z > 0.004$) and the strong hydrogen-shell flash (mainly for $Z \leq 0.004$). When $Z > 0.004$, the systems above the boundaries have mass ratios too large to stabilize mass transfer. If $Z \leq 0.004$, the mass transfer for the systems above the boundaries may be dynamically stable, but the mass-transfer rate is so high that most of the transferred material is lost from the system by the optically thick wind. The mass-transfer rate then sharply decreases to less than $\frac{1}{8}\dot{M}_{\text{cr}}$ after mass ratio inversion. The lower boundaries are constrained by the condition that the mass transfer rate is larger than $\frac{1}{8}\dot{M}_{\text{cr}}$ and that the secondaries have enough material to transfer onto CO WDs, which can then increase their masses to $1.378 M_{\odot}$.

We show the contours in the $(\log P^i, M_2^i)$ plane for four CO WD masses with various metallicities in Fig. 4, from which we may see the influence of metallicity. The results of other initial CO WD masses are similar to Fig. 4. We see that, with the increasing Z , the contour moves from lower left to upper right in the $(\log P^i, M_2^i)$ plane, indicating that the progenitor systems have more massive companions and longer orbital periods for a higher Z . This is due to the correlation between stellar structure and metallicity. Generally, high metallicity leads to larger radii of ZAMS stars, then the left hand boundary moves to longer initial orbital periods. Meanwhile, stars with high metallicity evolve in a way similar to those with low metallicity but less mass (Umeda et al. 1999; Chen & Tout 2007). Thus, for binaries of CO WDs with particular orbital periods, the companion mass increases with metallicity. The situation for the right hand boundaries is a bit complicated. They move slightly to a longer period with Z when $Z \geq 0.04$, while the tendency is reversed when $Z < 0.04$. This non-monotonic phenomenon is derived from the effect of composition (determined from equation 1) on opacity and, consequently, on stellar structure and evolution. For example, with increasing Z , the radius of a star at the base of RGB decreases when $Z < 0.04$, but increases when $Z \geq 0.04$ (Chen & Tout 2007; see Meng et al. 2008 for details about the effect of equation (1) on stellar evolution).

3.2 The minimum mass of the CO WD for which the WD+MS can produce a SN Ia

Previous studies show that the minimum mass of CO WDs leading to SNe Ia, $M_{\text{WD}}^{\text{min}}$, may be as low as $0.70M_{\odot}$ for $Z = 0.02$ (Langer et al. 2000; Han & Podsiadlowski 2004). In our study, $M_{\text{WD}}^{\text{min}}$ strongly depends on Z , as shown in Fig. 5. The relation between $M_{\text{WD}}^{\text{min}}$ and $\log(Z/Z_{\odot})$ is almost linear, and is fitted by

$$M_{\text{WD}}^{\text{min}}/M_{\odot} = 0.6679 - 0.08799 \log(Z/Z_{\odot}), \quad (13)$$

¹ Systems consisting of a low-mass secondary and a high-mass WD possibly undergo dynamically stable mass transfer at the base of the RGB and even on the RGB because of the low mass ratio. These systems may also contribute to SNe Ia (WD + RG). Since the study of WD + RG is beyond the scope of this paper, we leave out these systems from the contours.

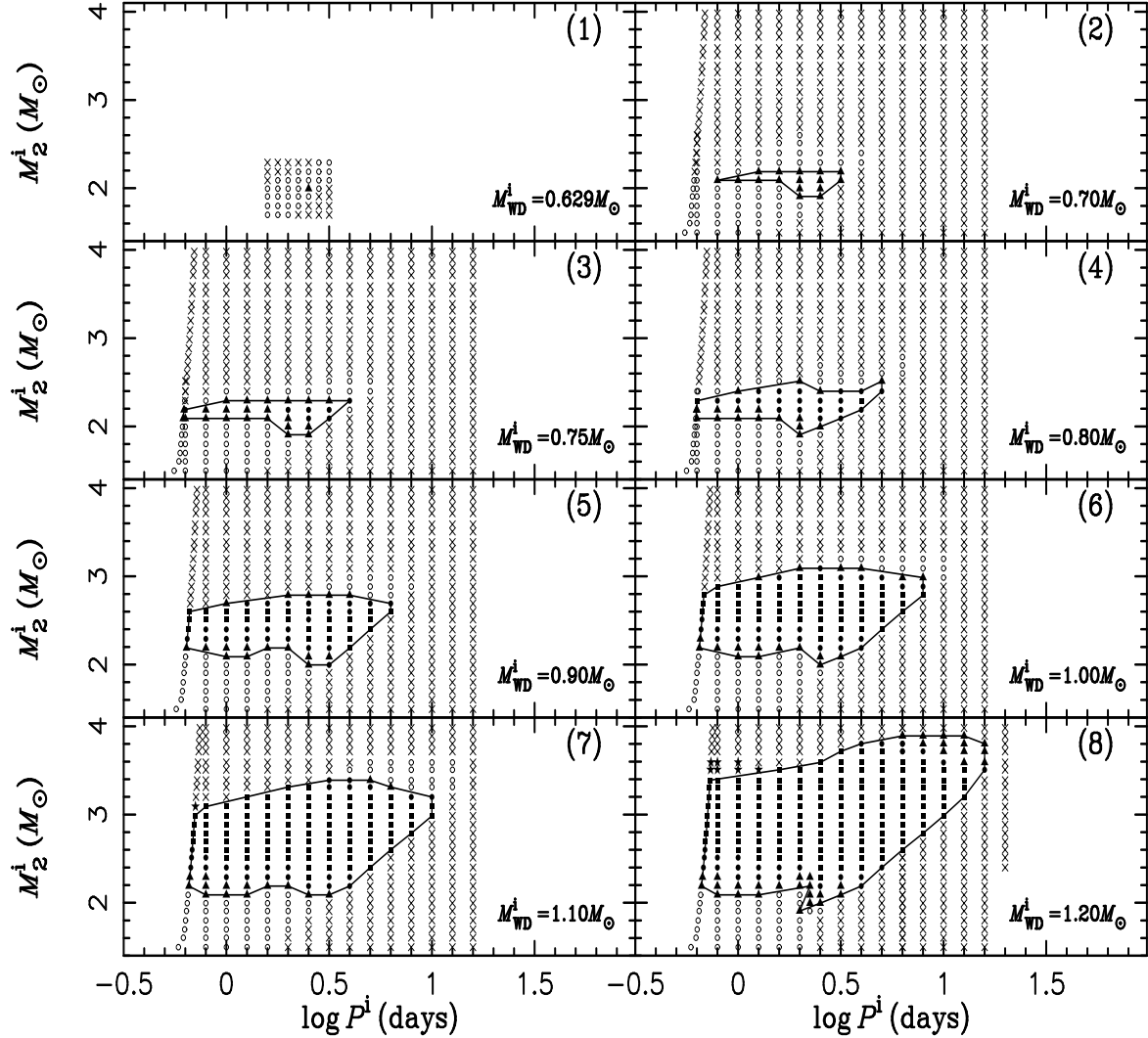


Figure 2. Final outcomes of binary evolution calculation in the initial orbital period-secondary mass ($\log P^i, M_2^i$) plane for CO WD + MS binaries with $Z = 0.06$, where P^i is the initial orbital period and M_2^i is the initial mass of donor star (for different initial WD masses as indicated in each panel). Filled squares indicate SN Ia explosions during an optically thick wind phase ($|\dot{M}_2| > \dot{M}_{\text{cr}}$). Filled circles denote SN Ia explosions after the wind phase, where hydrogen-shell burning is stable ($\dot{M}_{\text{cr}} \geq |\dot{M}_2| \geq \frac{1}{2}\dot{M}_{\text{cr}}$). Filled triangles denote SN Ia explosions after the wind phase where hydrogen-shell burning is mildly unstable ($\frac{1}{2}\dot{M}_{\text{cr}} > |\dot{M}_2| \geq \frac{1}{8}\dot{M}_{\text{cr}}$). Filled stars denote SN Ia explosions at delayed dynamical instability phase as shown in Han & Podsiadlowski (2006). Open circles indicate systems that experience nova explosion, preventing the CO WD from reaching $1.378 M_{\odot}$, while crosses show the systems that are unstable to dynamical mass transfer.

where the relative error of $M_{\text{WD}}^{\text{min}}$ is less than 2.3% in the fitting. We see in Fig. 5 that the minimum mass sharply decreases with metallicity and the difference in $M_{\text{WD}}^{\text{min}}$ between the cases of $Z = 0.06$ and $Z = 0.0001$ may be up to $0.24 M_{\odot}$. We explain this as follows: As mentioned in subsection 3.1, for a high Z , the companions in WD + MS systems for SNe Ia are more massive, and so have more material to transfer onto CO WDs. The CO WDs therefore do not need to be as massive for the production of SNe Ia. Meanwhile, the time-scale for mass transfer is the thermal time-scale,

which increases with metallicity. This leads to a lower mass-transfer rate for a high metallicity. As a consequence, less material is lost via optically thick wind. This means that a larger fraction of material can be accumulated on the surfaces of CO WDs for systems with a high Z . Therefore CO WDs can be initially less massive for SNe Ia for high Z .

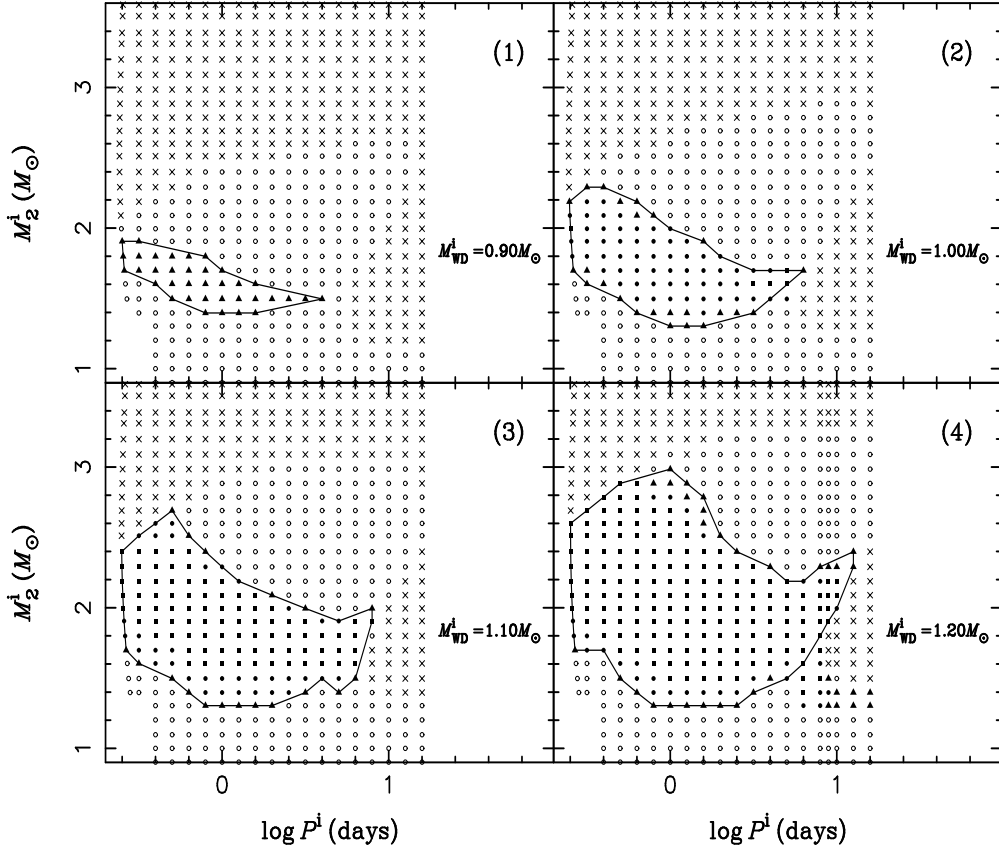


Figure 3. Similar to Fig 2 but for $Z = 0.0001$. In this figure, we do not plot the cases with minimum WD mass for simplicity of appearance of the figure. The minimum WD mass is $M_{WD}^{\min} = 0.860 M_{\odot}$ for $Z = 0.0001$. Out of the region surrounded by the solid line in panel (4), there are some filled symbols representing SNe Ia explosions. We do not include them in the contour since the mass transfer for these systems occurs on the giant branch or at the bottom of the giant branch (see footnote 1).

4 BINARY POPULATION SYNTHESIS

Adopting the results in section 3, we have studied the supernova frequency from the WD+MS channel via the rapid binary evolution code developed by Hurley et al. (2000, 2002). Here after, we use *primordial* to represent the binaries before the formation of WD+MS systems and *initial* for WD+MS systems.

4.1 Common envelope in binary evolution

During binary evolution, the primordial mass ratio (primary to secondary) is crucial for the first mass transfer. If it is larger than a critical mass ratio, q_c , the first mass transfer is dynamically unstable and a common envelope (CE) forms (Paczynski 1976). The ratio q_c varies with the evolutionary state of the primordial primary at the onset of RLOF (Hjellming & Webbink 1987; Webbink 1988; Han et al. 2002; Podsiadlowski et al. 2002; Chen & Han 2008). In this study, we adopt $q_c = 4.0$ when the primary is on MS or HG. This value is supported by detailed binary evolution studies (Han et al. 2000; Chen & Han 2002, 2003). If the primordial primary is on FGB or AGB, we use

$$q_c = [1.67 - x + 2(\frac{M_{cl}^P}{M_1^P})^5]/2.13, \quad (14)$$

where M_{cl}^P is the core mass of primordial primary, and $x = d \ln R_1^P / d \ln M_1^P$ is the mass-radius exponent of primordial primary and varies with composition. If the mass donors (primaries) are naked helium giants, $q_c = 0.748$ based on equation (14) (see Hurley et al. 2002 for details).

Embedded in the CE is a “new” binary consisting of the dense core of the primordial primary and the primordial secondary. Due to frictional drag within the envelope, the orbit of the “new” binary decays and a large part of the orbital energy released in the spiral-in process is injected into the envelope (Livio & Soker 1988). Here, we assume that the CE is ejected if

$$\alpha_{CE} \Delta E_{orb} = |E_{bind}|, \quad (15)$$

where ΔE_{orb} is the orbital energy released, E_{bind} is the binding energy of CE, and α_{CE} is CE ejection efficiency (i.e. the fraction of the released orbital energy used to eject the CE). This criterion is known as standard α -formalism (Nelemans et al. 2000; Nelemans & Tout 2005). Since the internal energy in the envelope is not incorporated into the binding energy, α_{CE} may be greater than 1 (see Han, Podsiadlowski & Eggleton 1995 for details about

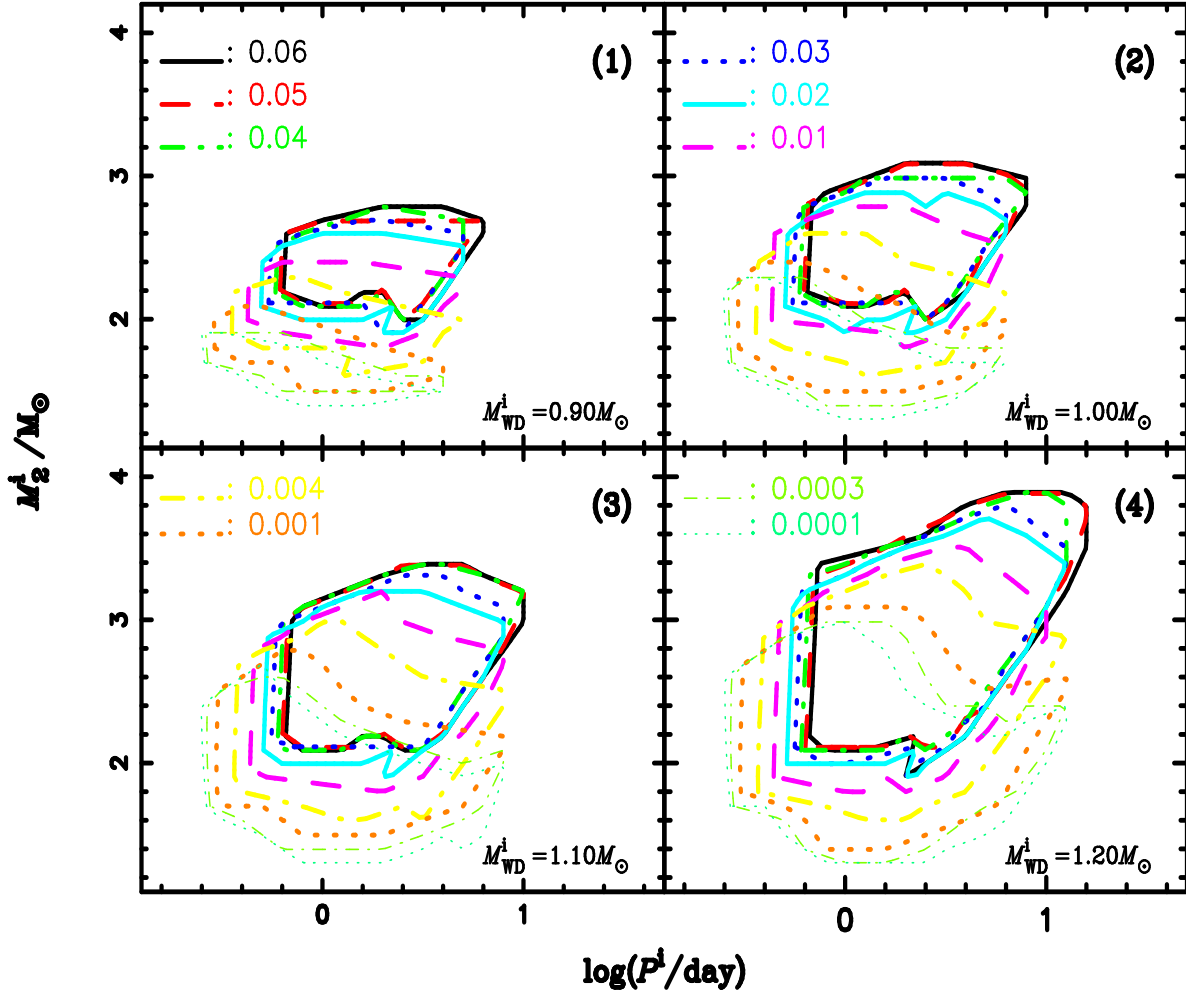


Figure 4. The contours of initial parameters in $(\log P^i, M_2^i)$ for different WD masses and different metallicities, in which SNe Ia are expected. The initial masses of WDs are shown in the lower-right region of each panel. Note that, in all the panels, we use the same types of lines, as indicated, to represent each metallicity.

the internal energy). In this paper, we set α_{CE} to be 1.0 or 3.0.

Nelemans et al. (2000) and Nelemans & Tout (2005) found that it is difficult for the standard α -formalism to reproduce a close pair of white dwarfs without the inclusion of the thermal energy of the envelope. They then suggested an alternative algorithm equating the angular momentum balance (the γ -algorithm, Nelemans & Tout 2005), which may explain the formation of all kinds of close binaries. However, Webbink (2007) argued that the α -formalism with envelope internal energy included can reproduce observations best. Note that the formation of WD + MS binaries is not much affected by the use of the γ -algorithm in comparison to α -formalism, especially when $\alpha_{\text{CE}} = 3.0$ (Nelemans & Tout 2005). Therefore, we continue to use the α -formalism throughout this paper and the main results in this paper will hold regardless.

4.2 Evolutionary channels to WD + MS systems

According to the evolutionary phase of the primordial primary at the onset of the first RLOF, WD + MS systems can be produced from three channels.

Case 1 (He star channel): the primordial primary is in HG or on RGB at the onset of the first RLOF (i.e. case B evolution defined by Kippenhahn & Weigert 1967). In this case, a CE is formed because of a large mass ratio or a convective envelope of the mass donor. After the CE ejection (if it occurs), the mass donor becomes a helium star and continues to evolve. The helium star likely fills its Roche lobe again after the central helium is exhausted. Since the mass donor is much less massive than before, this RLOF is dynamically stable, resulting in a close CO WD+MS system (see Nomoto et al. 1999, 2003 for details). The primordial orbital periods may range from 10 to 1000 days for this channel.

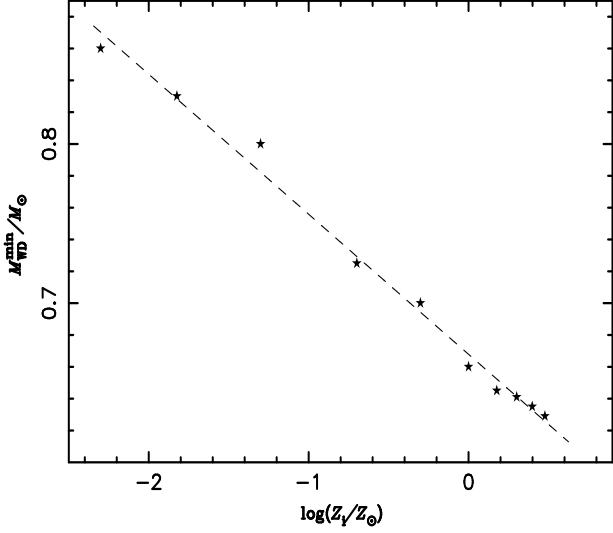


Figure 5. Relation between the minimum mass of CO WD for the production of SNe Ia and metallicity, with which the CO WD can increase its mass to $1.378 M_{\odot}$.

Case 2 (EAGB channel): the primordial primary is in early asymptotic giant branch stage (EAGB) (i.e. helium is exhausted in the core, while thermal pulses have not yet started). A CE is formed because of dynamically unstable mass transfer. After the CE is ejected, the orbit decays and the primordial primary becomes a helium red giant (HeRG). The HeRG may fill its Roche lobe and start the second RLOF. Similar to the He star channel, this RLOF is stable and produces WD + MS systems after RLOF. The range of the primordial periods is $\sim 100 - 1000$ days for this channel. During the EAGB, the hydrogen-burning shell is extinct in the primary, which has the same core mass as that at the bottom of the EAGB (Hurley et al. 2000).

Case 3 (TPAGB channel): the primordial primary fills its Roche lobe at the thermal pulsing AGB (TPAGB) stage. Similar to the above two channels, a CE is formed during the RLOF. A CO WD + MS binary is produced after CE ejection. The primordial periods of the systems experiencing the channel are larger than 1000 days.

Generally, the CO WD + MS binaries obtained from the different channels above have some different properties and these properties eventually determine whether the systems may explode as SNe Ia or not. We will discuss this in section 5. The WD + MS systems continue to evolve and the MS companions may fill their Roche lobes, and transfer their material to the CO WDs, which are likely to explode as SNe Ia. Here, we assume that, if the initial orbital period, P_{orb}^i , and the initial secondary mass, M_2^i , of a WD + MS system is located in the appropriate regions in the $(\log P^i, M_2^i)$ plane (see Figs. 2 to 3) for SNe Ia at the onset of RLOF, a SN Ia is produced.

4.3 Basic parameters for Monte Carlo simulations

To investigate the birth rate of SNe Ia, we followed the evolution of 10^7 binaries for various Z via Hurley's rapid binary evolution code (Hurley et al. 2000, 2002). The results of grid calculations in section 3 are incorporated into the code. The

code is only valid for $Z \leq 0.03$, and the production of SNe Ia of seven metallicities, i.e. $Z = 0.03, 0.02, 0.01, 0.004, 0.001, 0.0003$ and 0.0001 , are investigated here. The primordial binary samples are generated in a Monte Carlo way and a circular orbit is assumed for all binaries. The basic parameters for the simulations are as follows.

(i) The initial mass function (IFM) of Miller & Scalo (1979) is adopted. The primordial primary is generated according to the formula of Eggleton et al. (1989)

$$M_1^P = \frac{0.19X}{(1-X)^{0.75} + 0.032(1-X)^{0.25}}, \quad (16)$$

where X is a random number uniformly distributed in the range $[0,1]$ and M_1^P is the mass of the primordial primary, which ranges from $0.1 M_{\odot}$ to $100 M_{\odot}$.

(ii) The mass ratio of the primordial binaries, q' , is a very important parameter for binary evolution. For simplicity, we take a uniform mass-ratio distribution (Mazeh et al. 1992; Goldberg & Mazeh 1994):

$$n(q') = 1, \quad 0 < q' \leq 1, \quad (17)$$

where $q' = M_2^P / M_1^P$.

(iii) We assume that all stars are members of binary systems and that the distribution of separations is constant in $\log a$ for wide binaries, where a is separation, and falls off smoothly at small separation:

$$a \cdot n(a) = \begin{cases} \alpha_{\text{sep}}(a/a_0)^m & a \leq a_0; \\ \alpha_{\text{sep}}, & a_0 < a < a_1, \end{cases} \quad (18)$$

where $\alpha_{\text{sep}} \approx 0.070$, $a_0 = 10 R_{\odot}$, $a_1 = 5.75 \times 10^6 R_{\odot} = 0.13 \text{ pc}$ and $m \approx 1.2$. This distribution implies that the numbers of wide binary systems per logarithmic interval are equal, and that approximately 50 percent of the stellar systems have orbital periods less than 100 yr (Han, Podsiadlowski & Eggleton 1995).

(iv) We simply assume a single starburst (i.e. $10^{11} M_{\odot}$ in stars are produced one time) or a constant star formation rate S (SFR) over the last 15 Gyr calibrated so that one binary with $M_1 > 0.8 M_{\odot}$ is born in the Galaxy each year (see Iben & Tutukov 1984; Han, Podsiadlowski & Eggleton 1995; Hurley et al. 2002). From this calibration, we can get $S = 5 \text{ yr}^{-1}$ (see also Willems & Kolb 2004). The constant star formation rate is consistent with the estimation of Timmes et al. (1997), which successfully reproduces the ^{26}Al 1.809-MeV gamma-ray line and the core-collapse supernova rate in the Galaxy (Timmes et al. 1997).

5 THE RESULTS OF BINARY POPULATION SYNTHESIS

5.1 the Birth rates of SNe Ia

Fig. 6 shows the Galactic birth rates of SNe Ia (i.e. $Z = 0.02$ and $\text{SFR} = 5.0 M_{\odot}/\text{yr}$) from the WD+MS channel. From the figure, we see that the Galactic birth rate is around $0.7\text{--}1.0 \times 10^{-3} \text{ yr}^{-1}$, consistent with that of Han & Podsiadlowski (2004). This result is lower but comparable to that inferred from observations ($3\text{--}4 \times 10^{-3} \text{ yr}^{-1}$, van den Bergh & Tammann 1991; Cappellaro & Turatto 1997).

The birth rate of SNe Ia at various metallicities are presented in Fig. 7. In this figure, we see that most supernovae

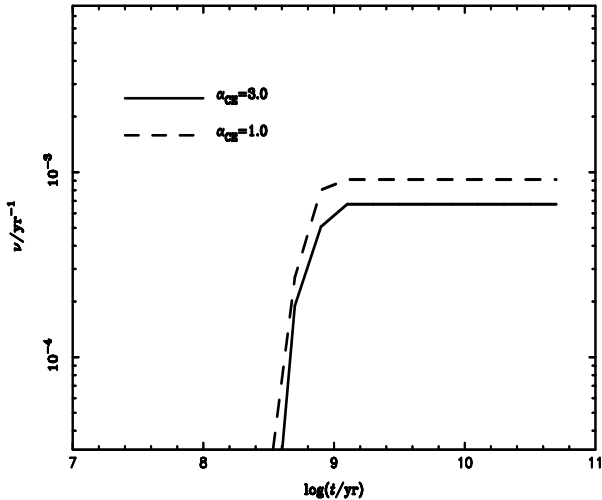


Figure 6. The evolution of the birth rates of SNe Ia for a constant star formation rate ($Z=0.02$, $\text{SFR}=5M_{\odot}\text{yr}^{-1}$). Solid and dashed lines show the cases with $\alpha_{\text{CE}} = 3.0$ and $\alpha_{\text{CE}} = 1.0$, respectively.

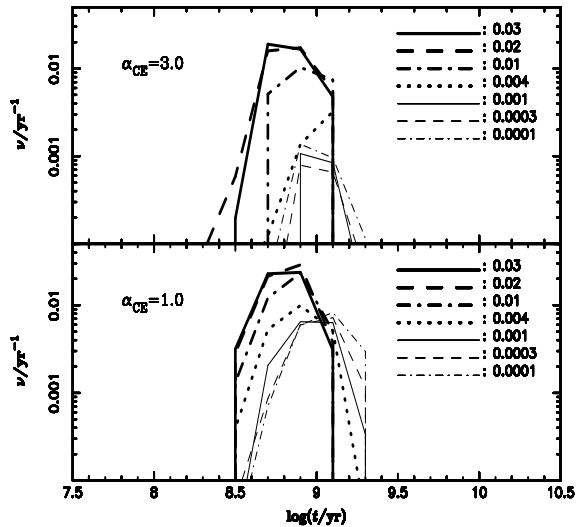


Figure 7. The evolution of the birth rates of SNe Ia for a single starburst of $10^{11}M_{\odot}$ for different metallicities. The upper panel shows the cases with $\alpha_{\text{CE}} = 3.0$, while the cases of $\alpha_{\text{CE}} = 1.0$ are in the bottom panel.

occur between 0.2 Gyr and 2 Gyr after the starburst. An interesting phenomenon is that a high metallicity leads to a systematically earlier explosion time of SNe Ia, which due to the effect of metallicity Z on the maximum initial mass of the companion for SNe Ia and on the stellar evolution. As shown in Fig. 4, M_2^i increases with metallicity Z . Generally, a massive star evolves more quickly than a low-mass one. So, the explosion time is earlier with Z from this view. Though a high Z also slows the evolution of a star down, its influence is much less than that of stellar mass based on detailed calculations of stellar evolution (Umeda et al. 1999; Chen & Tout 2007).

We also see in Fig. 7 that the peak value increases with metallicity Z . This comes from the fact that the parameter

space for SNe Ia increases with metallicity, e.g. the range of the initial masses of WDs is larger for a high metallicity. In the upper panel of Fig. 7, however, the peak value for the case of $Z = 0.0001$ is higher than that of $Z = 0.001$, which is mainly from the influence of α_{CE} and Z on the TPAGB channel (see subsection 5.2.1). α_{CE} significantly affects the peak values only at low metallicities, that is, the peak value of the birth rate is obviously larger for $\alpha_{\text{CE}} = 1.0$ in comparison to $\alpha_{\text{CE}} = 3.0$ when $Z < 0.004$. These phenomena originate from the influences of α_{CE} and metallicity on the He star channel and the TPAGB channel (see subsection 5.2.1 for details).

However, the results above are opposite to the recent study of Guo et al. (2008), where an analytic method was used (see also Hachisu et al. 1999a,b and Nomoto et al. 1999, 2003). Guo et al. (2008) found that the peak of the birth rate for a low Z appears significantly earlier than that for a high Z . Also, they have not found the dependence of the peak value of birth rate on metallicity. This discrepancy comes from the different approaches in calculating $|M_2|$ in the two studies. As described in section 2, the value of $|M_2|$ is crucial for the accretion of CO WDs. Thus, initial parameter spaces for SNe Ia are different in the two studies, i.e. a low metallicity leads to a higher maximum mass of the progenitors in Guo et al. (2008). This tendency is the opposite of that in this paper. Then, the delay times of SNe Ia, which are closely relevant to the initial companion mass, are also different. The final birth rates are therefore different. For example, given $Z = 0.02$, the peak value from the analytic method is larger than that from detailed binary evolution calculations by a factor of 3, if a single starburst is assumed (Han & Podsiadlowski 2004). Note that our results are more physical than those obtained from the simple analytic method used by Hachisu et al. (1999a,b), Nomoto et al. (1999, 2003) and Guo et al. (2008), as our results are based on detailed binary evolution calculations with the latest input physics.

5.2 Distribution of initial parameters of WD + MS systems for SNe Ia

Observationally, some WD + MS systems are possible progenitors of SNe Ia (see the review of Parthasarathy et al. 2007). Further studies are necessary to finally confirm them (from both observations and theories). In this section, we will present some properties of initial WD + MS systems for SNe Ia, which may help us to search for the potential progenitors of SNe Ia in various environments.

5.2.1 Distribution of initial masses of WDs

The distribution of initial WD masses from different channels are shown in Fig. 8, in which the relative importance of the three channels is clearly shown. In Fig. 9, we present the distribution of the initial masses of the CO WDs leading to SNe Ia for various Z and α_{CE} . Fig. 8 shows that α_{CE} is crucial for the He star channel. If a system experiences CE phase before rather than after helium burning, it will more likely merge due to a large binding energy and a short primordial orbital period, especially for $\alpha_{\text{CE}} = 1.0$. Thus, the contribution of WD + MS systems from the He star channel

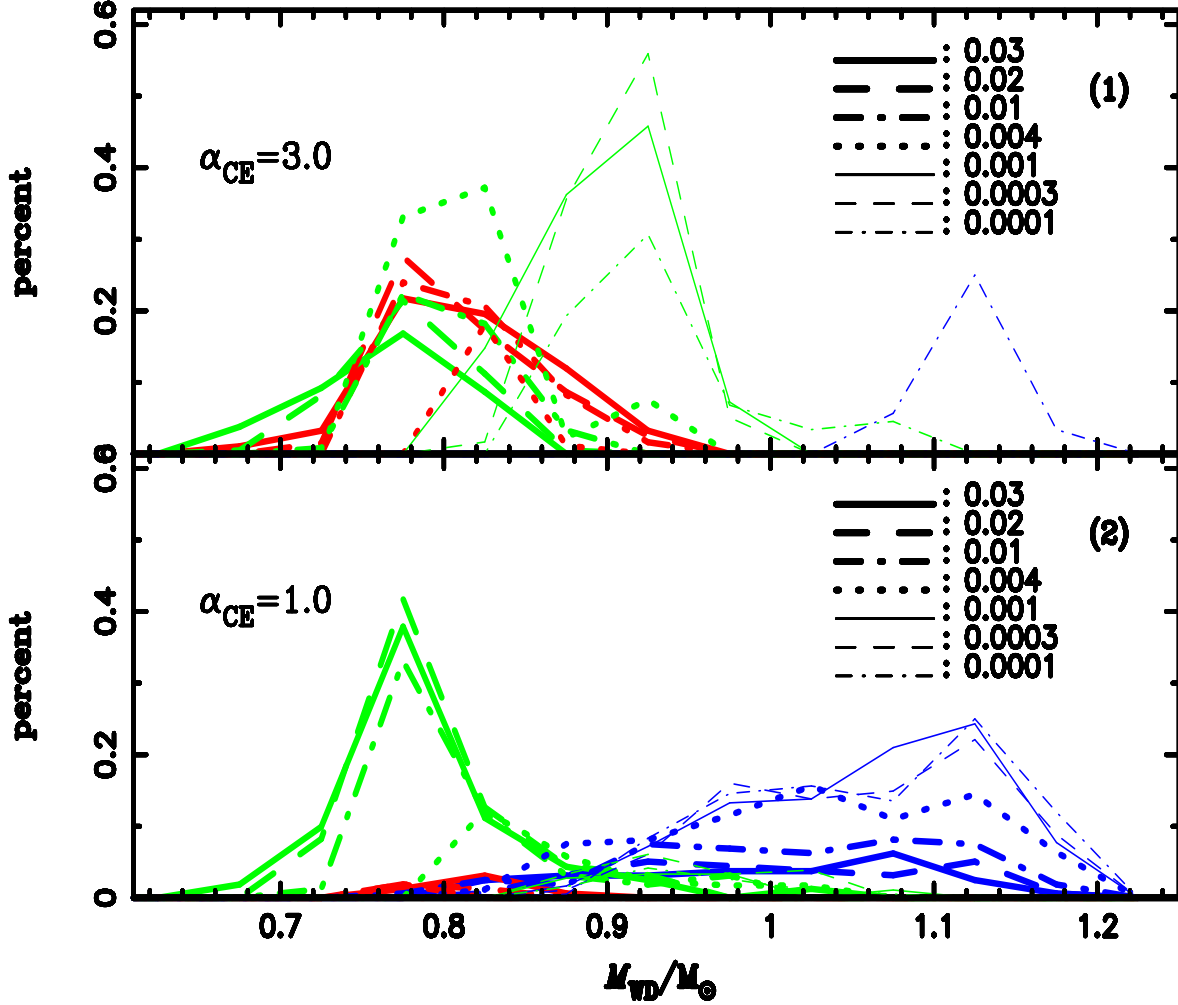


Figure 8. The distribution of the initial WD masses in WD + MS systems from different SN Ia channels for various metallicities and different α_{CE} . The red, green and blue lines represent those from He star, EAGB and TPAGB channel, respectively.

is less when $\alpha_{\text{CE}} = 1.0$ and increases when $\alpha_{\text{CE}} = 3.0$. Since the stellar radius increases with metallicity Z , a primordial binary with given M_1^{P} , M_2^{P} and P^{P} is more likely to undergo He star channel evolution if it has a high Z . The importance of the He star channel thus increases with metallicity Z . Actually, no WD + MS systems result from this channel when $Z < 0.004$ in our simulation. He star channel has an important contribution to WD + MS systems with CO WDs around $0.78M_{\odot}$ (see the peaks at low masses in Fig. 9).

The EAGB channel is **not** significantly influenced by α_{CE} for its moderate primordial orbital period, and it is the only contributor to the peaks at masses $\sim 0.92M_{\odot}$ in the upper panel of Fig. 9. EAGB channel also produces many WD + MS system with CO WD mass around $0.78M_{\odot}$ (see Fig 8).

The massive CO WDs (i.e the high-mass tail for $Z > 0.004$, the plateau from $0.9M_{\odot}$ to $1.20M_{\odot}$ for $Z \leq 0.004$ with $\alpha_{\text{CE}} = 1.0$, and peak around $1.13M_{\odot}$ with $\alpha_{\text{CE}} = 3.0$

and $Z = 0.0001$ in Fig. 9) are mainly from TPAGB channel (see the blue lines in Fig. 8). Because of the low binding energy of the common envelope and a long primordial orbital period, α_{CE} has a remarkable influence on CO+WD systems from the TPAGB channel. Generally, if a CE can be ejected, a low α_{CE} produces a shorter orbital-period WD + MS system, which is more likely to fulfill the conditions for SNe Ia. Therefore, we see obvious contributions from the TPAGB channel when $\alpha_{\text{CE}} = 1.0$, but no contribution from this channel when $\alpha_{\text{CE}} = 3.0$ except for the case of $Z = 0.0001$. We explain this as follows: For a low Z , due to relatively small stellar radius, binaries undergoing TPAGB channels usually have shorter primordial orbital periods and tighter common envelopes, and the produced CO WD + MS binaries have shorter orbital periods after CE ejection and are more likely to contribute to SNe Ia. This effect increases with the decrease of metallicity. We therefore see the high-mass peak in the figure for metallicity as low as 0.0001 with

$\alpha_{\text{CE}} = 3.0$. It is a little bit different with $\alpha_{\text{CE}} = 1.0$, for which the produced WD + MS systems have shorter initial orbital periods in comparison to $\alpha_{\text{CE}} = 3.0$. Thus, many WD + MS systems, which can not lead to SNe Ia with $\alpha_{\text{CE}} = 3.0$, contribute to SNe Ia with $\alpha_{\text{CE}} = 1.0$, and produce a plateau of CO WD masses instead of a peak (the bottom panel in Fig. 9).

As discussed above, for high Z , the contribution to SNe Ia from the He star channel increases, while that from the TPAGB channel decreases with α_{CE} , which leads to a nearly constant birth rate of SNe Ia for different values of α_{CE} . However, for the cases with low metallicities, the He star channel has no contribution to SNe Ia at either value adopted for α_{CE} , while a large amount of WD + MS systems from the TPAGB channel contribute to SNe Ia at the low α_{CE} , resulting in a higher birth rate in comparison to the high α_{CE} .

5.2.2 Distribution of initial secondary masses

Fig. 10 presents the distributions of the initial masses of secondaries for SNe Ia for various metallicity Z and α_{CE} . The distributions for different metallicities have similar shapes (i.e. a low-mass sharp peak with a high-mass tail). Since the contours for SNe Ia move to higher masses with Z , the peak mass of the secondaries also moves to higher masses with Z . The difference of the peak initial masses of the secondaries between $Z = 0.03$ and $Z = 0.0001$ is as large as $\sim 0.7M_{\odot}$.

5.2.3 Distribution of initial orbital periods

The distributions of the initial orbital periods are shown in Fig. 11. Similar to the distribution of initial masses of CO WDs, there are also double peaks for $Z = 0.0001$ and $\alpha_{\text{CE}} = 3.0$, which correspond to the low-mass peak and the high-mass one in Fig. 9, respectively.

5.2.4 Distribution of initial separations

The distributions of the initial separations are shown in Fig. 12. Similar to the distributions of the initial masses of CO WDs and that of the initial orbital periods, there are double peaks for the case of $Z = 0.0001$ and $\alpha_{\text{CE}} = 3.0$. The low-separation peak is from EAGB channel and the high-separation one is from TPAGB channel.

We see from Fig. 12 that there are almost no initial systems with separations larger than $\sim 26R_{\odot}$. This is a natural result since we only focus on WD + MS systems in this paper. For systems with long initial separations, mass transfer occurs on RGB, which is beyond the scope of this paper.

6 DISCUSSION

6.1 Correlation between the peak luminosity of SNe Ia and metallicity

In our study, the masses of CO WDs leading to SNe Ia are more massive in a low-metallicity environment (see Figs 5 and 9). Some previous studies showed that a massive CO WD leads to a lower C/O ratio, and thus a lower

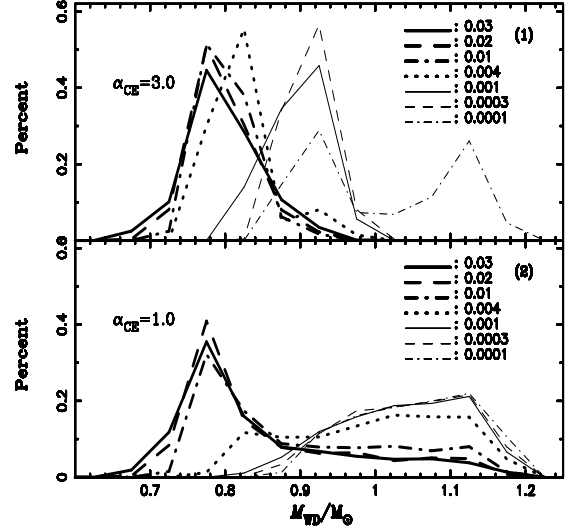


Figure 9. The distribution of the initial WD masses in WD + MS systems which can ultimately produce SNe Ia for various metallicities and different α_{CE} .

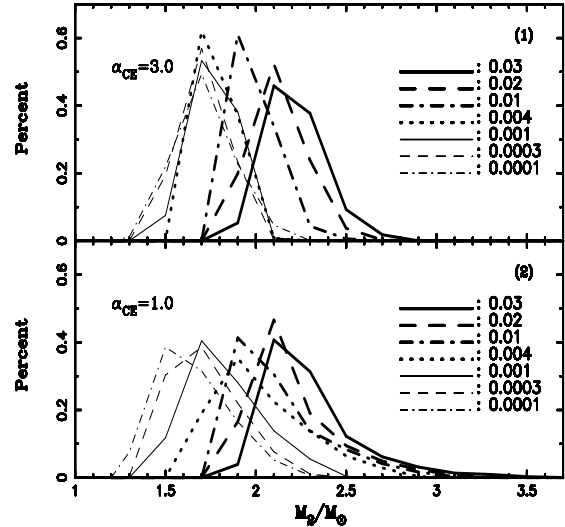


Figure 10. The distribution of the initial masses of secondaries in WD + MS systems which can ultimately produce SNe Ia for different metallicities and different α_{CE} .

amount of ^{56}Ni synthesized in the thermonuclear explosion (Nomoto et al. 1999, 2003), which results in a lower luminosity of SNe Ia (Arnett 1982; Arnett, Branch & Wheeler 1985; Branch 1992). According to this, our results means that the mean maximum luminosity of SNe Ia increases with metallicity Z , implying that the average maximum luminosity decreases with redshift, since metallicity generally decreases with redshift. Observationally, the mean peak brightness of SNe Ia in a galaxy has less variation in the outer regions than in the inner regions (Wang et al. 1997; Riess et al. 1999). Nomoto et al. (1999, 2003) suggested that this results from the effect of metallicity, i.e. the maximum peak brightness of SNe Ia is larger in the inner region than that in the outer region of a galaxy since metallicity decreases along the radial direction of a galaxy (Baes et al. 2007; Lemasle et al.

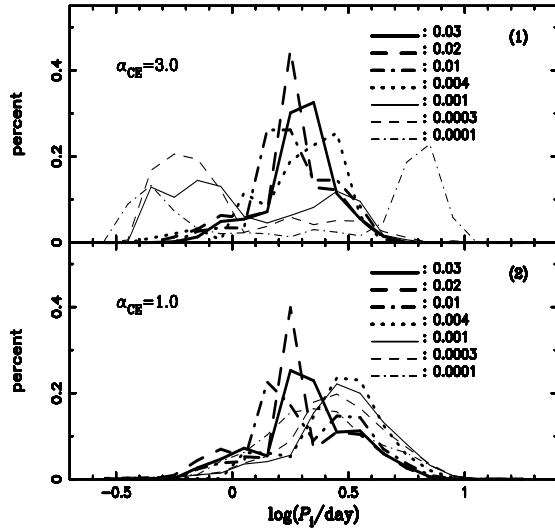


Figure 11. The distribution of the initial orbital periods of the WD+MS systems which can ultimately produce SNe Ia for different metallicities and different α_{CE} .

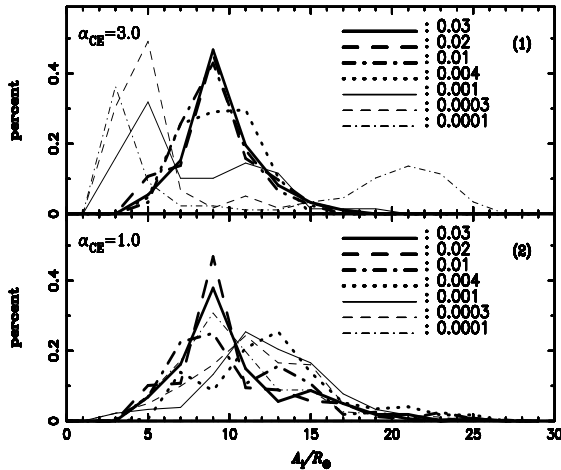


Figure 12. The distribution of the initial separations of the WD+MS systems which can ultimately produce SNe Ia for different metallicities and different α_{CE} .

2007), while the minimum peak brightness of SNe Ia is similar because the maximum initial CO WD mass is almost equal, i.e. $\sim 1.2 M_{\odot}$ (see Fig. 9 in this paper and Fig. 1 in Meng et al. 2008), which leads to the lowest C/O ratio of a CO WD and thus the least amount of ^{56}Ni synthesized in the thermonuclear explosion (Nomoto et al. 1999, 2003). In addition, Hamuy et al. (1996b) did not find the classical Malmquist bias in their sample and the most distant SNe Ia are not significantly brighter than nearby samples. This phenomenon is at least not inconsistent with our prediction.

Langer et al. (2000) suggested that on average, the initial masses of CO WDs for SNe Ia with a low metallicity ($Z = 0.001$) is larger than that with a high metallicity ($Z = 0.02$) by about $0.2 M_{\odot}$. From the BPS study in this paper, the difference of the CO WD masses from various metal-

licities may be up to $0.3 M_{\odot}$ (see Fig 9), consistent with the suggestion of Langer et al. (2000). Detailed single stellar evolution calculations (Han, Podsiadlowski & Eggleton 1994; Girardi et al. 2000; Meng et al. 2008) show that, for a given main-sequence star, the CO WD mass decreases with metallicity Z , that is, a $0.2 M_{\odot}$ difference of CO WD masses can be obtained from different metallicities (Meng et al. 2008). Since the CO WD masses from single stellar evolution may be taken as upper limits of CO WD masses from binary evolution to some extent, the mass difference of CO WDs for SNe Ia from different metallicities might be achieved from the evolution prior to CO WD formation.

6.2 Other possible channels for SNe Ia

From our study, the WD + MS channel can only account for about 1/3 of the SNe Ia observed (van den Bergh & Tammann 1991; Cappellaro & Turatto 1997). Therefore, there may be other channels or mechanisms contributing to SNe Ia. As mentioned in section 1, a wide symbiotic system, WD + RG, is a possible progenitor of SNe Ia (Hachisu et al. 1999b), though previous BPS studies indicated little contributions from this channel (Yungelson & Livio 1998; Han & Podsiadlowski 2004). Recently, Hachisu & Kato (2005, 2006a,b) and Hachisu et al. (2007) suggested that several recurrent novae are probable progenitors of SNe Ia and some of them belong to the WD+RG channel. Meanwhile, Patat et al. (2007) suggested that the companion of the progenitor of SN 2006X may be an early RGB star. So, a further study of this channel is necessary. An alternative is the double-degenerate (DD) channel (Iben & Tutukov 1984; Whelan & Iben 1987), although it is theoretically less favored (Hillebrandt & Niemeyer 2000). In this channel, two CO WDs with a total mass larger than the Chandrasekhar mass limit may coalesce and explode as a SN Ia. The birth rate from this channel is comparable to the observational value (Han 1998; Yungelson & Livio 1998, 2000; Tutukov & Yungelson 2002), and SN 2003fg and SN 2005hj likely resulted from the DD channel (Howell et al. 2006; Branch 2006; Quimby, Höflich & Wheeler 2007). Observationally, a large amount of DD systems are discovered (Napiwotzki et al. 2004), but only KPD 1930+2752 is a possible progenitor candidate for a SN Ia via DD channel (Geier et al. 2007). The total mass of KPD 1930+2752 ($\sim 1.52 M_{\odot}$) exceeds the Chandrasekhar mass limit and the time scale of coalescence is about 200 Myr estimated from orbital shrinkage caused by gravitational wave radiation (Geier et al. 2007). However, Ergma, Fedorova & Yungelson (2001) argued that, from detailed binary evolution calculation, the final mass of KPD 1930+2752 is smaller than the Chandrasekhar mass limit due to a large amount of mass loss during evolution. In addition, earlier numerical simulations showed that the most probable fate of the coalescence is an accretion-induced collapse and, finally, neutron star formation (see the review by Hillebrandt & Niemeyer 2000). A definitive conclusion for DD model is thus premature at present, and further studies are needed.

Liebert et al. (2003, 2005) and Wickramasinghe & Ferrario (2005) found that about 10% of WDs have magnetic fields higher than 1 MG. The mean mass of these WDs is $0.93 M_{\odot}$, compared to mean

mass of all WDs which is $0.56 M_{\odot}$ (see the review by Parthasarathy et al. 2007 for details). Thus, the magnetic WDs are more likely to reach the Chandrasekhar mass limit by accretion. Meanwhile, the magnetic field may also affect some properties of WD+MS systems, e.g. the mass transfer rate, the critical accretion rate, the thermonuclear reaction rate etc, leading to a different birth rate of SNe Ia.

6.3 2002ic-like supernovae

Until SN 2002ic was discovered (Hamuy et al. 2003), it was long believed that there are no hydrogen lines in the spectra of SNe Ia. The strong hydrogen lines in the spectra of SN 2002ic were explained by the interaction between the SN ejecta and the circumstellar material (CSM) (Hamuy et al. 2003). The CSM is aspheric around the SN Ia from spectropolarimetry data (Deng et al. 2004; Wang et al. 2004) and has a mass of $0.5\text{--}6M_{\odot}$ (Wang et al. 2004; Chugai & Yungelson 2004; Uenishi et al. 2004; Kotak et al. 2004). The shape of the light curve showed that there was a delay between the explosion and the interaction, indicating a cavity between the progenitor and the CSM (Wood-Vasey et al. 2004; Wood-Vasey & Sokoloski 2006). Recently, two co-twins of SN 2002ic (SN 2005gj and SN 2006gy) were also found (Aldering et al. 2006; Ofek et al. 2007). Benetti et al. (2006) argued that SN 2002ic is not a Type Ia supernova, but a Type Ic SN surrounded by a structured H-rich CSM, possibly asymmetric. However, recent spectral comparison between SN 2005gj, SN 2002ic and SNe Ia provided further evidence of Type Ia rather than Ic for SN 2002ic (Prieto et al. 2007). Thus, we still take SN 2002ic as a SN Ia. To explain these rare objects, many models were suggested and here we just list some of them: Hachisu et al. 1999b; Hamuy et al. 2003; Livio & Riess 2003; Chugai & Yungelson 2004; Han & Podsiadlowski 2006.

Among all the models listed above, the model of Han & Podsiadlowski (2006) is the best model to match with the observation at present, especially about the birth rate of these rare objects and the delay time (Aldering et al. 2006; Prieto et al. 2007). In the scenario of Han & Podsiadlowski (2006), SN 2002ic might be from the WD + MS channel, where the CO WD accretes material from its relatively massive companion ($\sim 3.0M_{\odot}$), and increases its mass to $\sim 1.30M_{\odot}$ before experiencing a delayed dynamical instability. From this scenario, we examined the initial parameters for 2002ic-like SNe Ia by assuming that the CO WD can increase its mass to $1.378 M_{\odot}$ and explode as a SN 2002ic-like case if the mass of the CO WD exceeds $1.30 M_{\odot}$ before the delayed dynamical instability. As shown in Figs. 2 and 3², the parameter space for the SN 2002ic-like case becomes larger with metallicity. For $Z = 0.0001$, no systems become 2002ic-like supernovae. This means that *the SN 2002ic-like case could not occur in extremely low-metallicity environments if the model in Han & Podsiadlowski (2006) is appropriate*. Observationally, the host galaxy of SN 2006gy has a solar metallicity, while there is no information on the metallicity of SN 2002ic since any association between SN

2002ic and the galaxies near SN 2002ic have been ruled out (Hamuy et al. 2003; Kotak et al. 2004). However, we may speculate that the metallicity of SN 2002ic is likely to be higher than 0.0001 from the redshift of $z = 0.066$. For the host galaxy of SN 2005gj, we only know $Z/Z_{\odot} < 0.3$ (Aldering et al. 2006), which might not be as low as 0.0001. Our model predicts that no SN 2002ic-like events would be observed in extremely low metallicity environments or at very high redshift, which can be tested with an enlarged sample of 2002ic-like supernova in the future.

7 SUMMARY AND CONCLUSION

Adopting the prescription of Hachisu et al. (1999a) for the mass accretion of CO WDs and assuming that the prescription is valid for all metallicities, we have studied the progenitors of SNe Ia in the single degenerate channel (WD+MS) via detailed binary evolution calculations. The initial parameters for SNe Ia in the $(\log P^i, M_2^i)$ plane are obtained for ten metallicities. One can download the FORTRAN code for the contours leading to SNe Ia at <http://www.ynao.ac.cn/~bps/download/xiangcunmeng.htm>.

We found that the contours for SNe Ia move to high mass and long orbital period with increasing metallicity. The minimum initial mass of the CO WDs for SNe Ia sharply decreases with metallicity and the difference of the minimum initial mass between $Z = 0.06$ and $Z = 0.0001$ is as large as $0.24 M_{\odot}$. Incorporating the binary evolution calculation results in this paper into Hurley's rapid binary evolution code, we have studied the evolution of the birth rates of SNe Ia with time. The Galactic birth rate from the WD+MS channel is lower than but still comparable, within a factor of a few, to that inferred from observations. For the cases of a single starburst, the SNe Ia explosions occur earlier and the peak value of the birth rate is larger for a high metallicity. The distributions of the initial masses of CO WDs, the initial masses of secondaries, the initial periods and the initial separations evolve significantly with metallicity. Based on the model of Han & Podsiadlowski (2006), we predict that 2002ic-like supernovae would not occur in extremely low-metallicity environments.

ACKNOWLEDGMENTS

We thank Dr. Richard Pokorný for his kind help in improving the language of this paper. This work was in part supported by Natural Science Foundation of China under Grant Nos. 10433030, 10521001, 2007CB815406 and 10603013.

REFERENCES

- Aldering G., Antilogus P., Bailey S. et al., 2006, ApJ, 650, 510
- Alexander D. R., Ferguson J. W., 1994, ApJ, 437, 879
- Arnett W.D., 1982, ApJ, 253, 785
- Arnett, W.D., Branch, D., Wheeler, J.C., 1985, Nature, 314, 337
- Baes M., Sil'chenko O.K., Moiseev A.V. et al., 2007, A&A, 467, 991

² See my personal web site <http://www.ynao.ac.cn/~bps/download/xiangcunmeng.htm> to see the cases with other metallicities.

- Benetti S., Cappellaro E., Turatto M. et al., 2006, *ApJ*, 653, L129
- Branch D., 1992, *ApJ*, 392, 35
- Branch D., Bergh S.V., 1993, *AJ*, 105, 2231
- Branch D., 2004, *Nature*, 431, 1044
- Branch D., 2006, *Nature*, 443, 283
- Cappellaro E., Turatto M., Tsvetkov D.Y., Bartunov O.S., Pollas C., Evans R., Hamuy M., 1997, *A&A*, 322, 431
- Cappellaro E., Turatto M., 1997, in Ruiz-Lapuente P., Canal R., Isern J., eds, *Thermonuclear Supernovae*. Kluwer, Dordrecht, p. 77
- Chugai N.N., Yungelson L.R., 2004, *Astronomy Letters*, 30, 65
- Chen X., Han, Z., 2002, *MNRAS*, 335, 948
- Chen X., Han, Z., 2003, *MNRAS*, 341, 662
- Chen X., Tout C.A., 2007, *ChJAA*, 7, 2, 245
- Chen X., Han, Z., 2008, *MNRAS*, 387, 1416, arXiv: 0804.2294
- Deng J., Kawabata K.S., Ohya Y. et al., 2004, *ApJ*, 605, L37
- Di Stefano R., Kong A.K.H., 2003, *ApJ*, 592, 884
- Eggleton P.P., 1971, *MNRAS*, 151, 351
- Eggleton P.P., 1972, *MNRAS*, 156, 361
- Eggleton P.P., 1973, *MNRAS*, 163, 279
- Eggleton P. P., Tout C. A., Fitchett M. J., 1989, *ApJ*, 347, 998
- Ergma E., Fedorova A.V., Yungelson L.R., 2001, *A&A*, 376, L9
- Guo W., Zhang F., Meng X., Li Z., Han Z., 2008, *ChJAA*, 8, 63
- Geier S., Nesslinger S., Heber U., Przybilla N., Napiwotzki R., Kudritzki R.-P., 2007, *A&A*, 464, 299
- Girardi L., Bressan A., Bertelli G., 2000, *A&A*, 141, 371
- Goldberg D., Mazeh T., 1994, *A&A*, 282, 801
- Hachisu I., Kato M., Nomoto K., *ApJ*, 1996, 470, L97
- Hachisu I., Kato M., Nomoto K., Umeda H., 1999a, *ApJ*, 519, 314
- Hachisu I., Kato M., Nomoto K., 1999b, *ApJ*, 522, 487
- Hachisu I., Kato M., 2003a, *ApJ*, 588, 1003
- Hachisu I., Kato M., 2003b, *ApJ*, 590, 445
- Hachisu I., Kato M., 2005, *ApJ*, 631, 1094
- Hachisu I., Kato M., 2006a, *ApJ*, 642, L52
- Hachisu I., Kato M., 2006b, *ApJ*, 651, L141
- Hachisu I., Kato M., Luna G.J.M., 2007, *ApJ*, 659, L153
- Hachisu I., Kato M., Nomoto K., 2008, *ApJ*, inpress, (arXiv: 0710.0319)
- Hamuy M., Phillips M.M., Schommer R.A., Schommer R.A., Suntzeff N.B., Maza J., Avilés R., 1996, *AJ*, 112, 2391
- Hamuy M., Phillips M.M., Suntzeff N.B., Schommer R.A. 1996b, *AJ*, 112, 2398
- Hamuy M. et al., 2003, *Nature*, 424, 651
- Han Z., Podsiadlowski P., Eggleton P.P., 1994, *MNRAS*, 270, 121
- Han Z., Podsiadlowski P., Eggleton P.P., 1995, *MNRAS*, 272, 800
- Han Z., 1998, *MNRAS*, 296, 1019
- Han Z., Tout C.A., Eggleton P.P., 2000, *MNRAS*, 319, 215
- Han Z., Podsiadlowski Ph., Maxted P. F. L., Marsh T. R., Ivanova N., 2002, *MNRAS*, 336, 449
- Han Z., Podsiadlowski Ph., 2004, *MNRAS*, 350, 1301
- Han Z., Podsiadlowski Ph., 2006, *MNRAS*, 368, 1095
- Hillebrandt W., Niemeyer J.C., 2000, *ARA&A*, 38, 191
- Hjellming M.S., Webbink R.F., 1987, *ApJ*, 318, 794
- Howell D.A. et al., 2006, *Nature*, 443, 308
- Hurley J.R., Pols O.R., Tout C.A., 2000, *MNRAS*, 315, 543
- Hurley J.R., Tout C.A., Pols O.R., 2002, *MNRAS*, 329, 897
- Iben I., Tutukov A.V., 1984, *ApJS*, 54, 335
- Iglesias C. A., Rogers F. J., 1996, *ApJ*, 464, 943
- Ihara Y., Ozaki J., Doi M. et al., 2007, *PASJ*, 59, 811, arXiv: 0706.3259
- Kato M., Hachisu I., 2004, *ApJ*, 613, L129
- Kippenhahn R., Weigert A., 1967, *ZA*, 65, 251
- Kobayashi C., Tsujimoto T., Nomoto K. et al., 1998, *ApJ*, 503, L155
- Kotak R., Meikle W.P.S., Adamson S. et al., 2004, *MNRAS*, 354, L13
- Langer N., Deutschmann A., Wellstein S. et al., 2000, *A&A*, 362, 1046
- Leibundgut B., 2000, *A&ARv*, 10, 179
- Lemasle B., Piersimoni A., Pedicelli P. et al., 2007, arXiv: 0711.3988
- Leonard D.C., 2007, *ApJ*, 670, 1275
- Li X.D., van den Heuvel E.P.J., 1997, *A&A*, 322, L9
- Liebert J., Bergeron P., Holberg J.B., 2003, *AJ*, 125, 348
- Liebert J., Bergeron P., Holberg J.B., 2005, *ApJS*, 156, 47
- Livio M., Soker N., 1988, *ApJ*, 329, 764
- Livio M., Riess A., 2003, *ApJ*, 594, L93
- Mannucci F., Della Valle M., Panagia N., Cappellaro E., Cresci G., Maiolino R., Petrosian A., Turatto M., 2005, *A&A*, 433, 807
- Mannucci F., Della Valle M., Panagia N., 2006, *MNRAS*, 370, 773
- Mattila S., Lundqvist P., Sollerman J. et al., 2005, *A&A*, 443, 649
- Mazeh T., Goldberg D., Duquennoy A., Mayor M., 1992, *ApJ*, 401, 265
- Meng X., Chen X., Tout C.A., Han Z., 2006, *ChJAA*, 6, 4, 461
- Meng X., Chen X., Han Z., 2008, *A&A*, 487, 625, arXiv: 0710.2397.
- Miller G.E., Scalo J.M., 1979, *ApJS*, 41, 513
- Napiwotzki R., Karl C., Nelemans G. et al., 2004, *RMxAC*, 20, 113
- Nelemans G., Verbunt F., Yungelson L.R. et al., 2000, *A&A*, 360, 1011
- Nelemans G., Tout C.A., 2005, *MNRAS*, 356, 753
- Nomoto K., Thielemann F.-K., Yokoi K., 1984, *ApJ*, 286, 644
- Nomoto K., Umeda H., Hachisu I. Kato M., Kobayashi C., Tsujimoto T., 1999, in Truran J., Niemeyer T., eds, *Type Ia Supernova :Theory and Cosmology*. Cambridge Univ. Press, New York, p.63
- Nomoto K., Uenishi T., Kobayashi C. Umeda H., Ohkubo T., Hachisu I., Kato M., 2003, in Hillebrandt W., Leibundgut B., eds, *From Twilight to Highlight: The Physics of supernova*, ESO/Springer serious “ESO Astrophysics Symposia” Berlin: Springer, p.115
- Ofek E.O., Cameron P.B., Kaslwal M.M. et al., 2007, *ApJ*, 659, L13, arXiv: 0612408
- Paczynski B., 1976, in Eggleton P.P., Mitton S., Whelan J., eds, *Structure and Evolution of Close Binaries*. Kluwer, Dordrecht, p. 75
- Parthasarathy M., Branch D., Jeffery D.J., Baron E., 2007,

- NewAR, 51, 524, arXiv: 0703415
- Patat E. et al., Science, 317, 924
- Podsiadlowski P., Rappaport S., Pfahl, 2002, ApJ, 565, 1107
- Podsiadlowski P., Mazzali P.A., Lesaffre P., Wolf C., Förster F., 2006, arXiv: 0608324
- Perlmutter S. et al., 1999, ApJ, 517, 565
- Phillips M.M., 1993, ApJ, 413, L105
- Pols O.R., Tout C.A., Eggleton P.P. et al., 1995, MNRAS, 274, 964
- Pols O.R., Tout C.A., Schröder K.P. et al., 1997, MNRAS, 289, 869
- Pols O.R., Schröder K.P., Hurly J.R. et al., 1998, MNRAS, 298, 525
- Prieto J.L. et al., 2008, ApJ, 673, 999, arXiv: 0707.0690
- Prieto J.L. et al., 2007, arXiv: 0706.4088
- Quimby R., P. Höflich, J.C. Wheeler, 2007, ApJ, 666, 1083
- Riess A. et al., 1999, AJ, 117, 707
- Riess A. et al., 1998, AJ, 116, 1009
- Ruiz-Lapuente P. et al., 2004, Nature, 431, 1069
- Scannapieco E., Bildsten L., 2005, ApJ, 629, L85
- Schröder K.P., Pols O.R., Eggleton P.P., 1997, MNRAS, 285, 696
- Shanks T., Allen P.D., Hoyle F. et al., 2002, ASPC, 283, 274
- Timmes F.X., Diehl R., Hartmann D.H., 1997, ApJ, 479, 760
- Timmes F.X., Brown E.F., Truran J.W., 2003, ApJ, 590, L83
- Travaglio C., Hillebrandt W., Reinecke M., 2005, A&A, 443, 1007
- Tutukov A.V., Yungelson L.R., 2002, Astron. Rep., 46, 667
- Totani T., Morokuma T., Oda T. et al., 2008, PASJ, 60, 1327, arXiv: 0804.0909
- Uenishi T., Suzuki T., Nomoto K. et al., 2004, Rev. Mex. A&A, 20, 219
- Umeda H., Nomoto K., Yamaoka H. et al., 1999, ApJ, 513, 861
- van den Bergh S., Tammann G.A., 1991, ARA&A, 29, 363
- Voss R., & Nelemans G., 2008, Nature, 451, 802
- Wang L., Höflich P., Wheeler J.C., 1997, ApJ, 483, L29
- Wang L., Baade D., Höflich P. et al., 2004, ApJ, 604, L53
- Webbink R. F., 1988, in The Symbiotic Phenomenon, eds. J. Mikolajewska, M. Friedjung, S. J. Kenyon & R. Viotti (Kluwer: Dordrecht), p.311
- Webbink R., 2007, arXiv: 0704.0280
- Whelan J., Iben I., 1973, ApJ, 186, 1007
- Whelan J., Iben I., 1987, in Philipp A.G.D., Hayes D.S., Liebert J.W., eds, IAU Colloq.95, Second Conference on Faint Blue Stars. Davis Press, Schenectady, p. 445
- Wickramasinghe D.T., Ferrario L., 2005, MNRAS, 356, 1576
- Willems B., Kolb U., 2004, A&A, 419, 1057
- Wood-Vasey W.M., Wang L., Aldering G., 2004, ApJ, 616, 339
- Wood-Vasey W.M., Sokoloski J.L., 2006, ApJ, 645, L53
- Yungelson L., Livio M., Tutukou A. Kenyon S.J., 1995, ApJ, 447, 656
- Yungelson L., Livio M., 1998, ApJ, 497, 168
- Yungelson L., Livio M., 2000, ApJ, 528, 108